ELEKTROTEHNIŠKI VESTNIK 85(4): 169-176, 2018
ORIGINAL SCIENTIFIC PAPER

Sensorless fuzzy sliding-mode control of the double-star induction motor using a sliding-mode observer

Mohamed Haithem Lazreg[1], Abderrahim Bentaallah[1]

[1] *Djillali Liabes University, Sidi Bel Abbes, Algeria.*
e-mail: haitem.31@hotmail.fr, bentaallah65@yahoo.fr

Abstract. The paper presents a sensorless fuzzy sliding-mode speed control (FSMC) decoupled by a vector control applied to a double-star induction motor (DSIM) using a sliding mode observer (SMO) fed by two PWM voltage source inverters. The fuzzy sliding-mode control is a hybrid control technique that links two control strategies, the sliding mode and fuzzy logic, whose sign function of the discontinuous part is replaced by a fuzzy inference system to overcome the drawbacks of the chattering phenomenon. For the control, the major problem is the need for using a mechanical sensor. Which imposes an additional cost and increases the complexity of the assembly. For this reason, we propose a sliding mode observer of a high robustness to few parametric uncertainties by providing considerable correction gains. The control + observer set is simulated by the Matlab / Simulink software and the simulation results show that its performance is robust and the chattering problem is solved.

Keywords: Double-star induction motor; Sliding-mode control; Fuzzy logic; Sensorless; Sliding-mode observer.

Brezsenzorsko mehko krmiljenje drsnega načina pri asinhronskem motorju z dvojnim statorskim navitjem

V prispevku smo predstavili hitro brezsenzorsko mehko krmiljenje drsnega načina pri asinhronskem motorju z dvojnim statorskim navitjem. Mehko krmiljenje drsnega načina je hibridna tehnika krmiljenja, ki združuje dva pristopa: drsni način in mehko logiko. Pri krmiljenju je največji problem uporaba mehanskega senzorja, ki povečuje kompleksnost izvedbe in ceno sistema. Ta problem smo rešili z uporabo observatorja drsnega načina. Predlagano rešitev smo simulirali s programskim orodjem Matlab/Simulink in rezultati simulacij potrjujejo njeno zmogljivost in robustnost.

1 INTRODUCTION

In order to provide electric motorization for high-power applications, such as rail traction or naval propulsion, it is often necessary to segment the power. The current solution apply segmentation at the ensembly level of the converter machines, by using multi-phase machines (machines with the number of phases greater than three). Indeed, multiplication of the number of phases allows splitting the power and thus reducing the switched voltages with given current. One of the most common examples of the multi-phase machines is the double-star induction motor (DSIM) [1].

The difficulty of control has encouraged the development of several control techniques so that these machines behave like the DC machines eliminating the coupling between the flux and torque [2], characterized by a natural decoupling of the flux and torque. One of these control techniques is the vector control. However, a disadvantage of controlling by using conventional control algorithms, such as PI controllers, is the machine sensitivity to parametric uncertainties and their variations [3]. To avoid this disadvantage, a robust sliding-mode adjustment technique is proposed. The sliding mode is a mode of the system operation with a variable structure. It is considered as one of the simplest approaches to control nonlinear systems and those having an imprecise model [4]. One of the notable advantage of this type of control is robustness to parameter variations. [5].

Fuzzy logic is one of the classes of artificial intelligence. Its purpose are the study and detection of imprecise knowledge and approximate reasoning [6]. It is complementary and used particularly when there is no precise mathematical model of the process to be controlled, or when the latter has strong nonlinearities or inaccuracies. To obtain a hybrid control, we combine these two techniques (fuzzy logic control and sliding-mode control). A chattering-free fuzzy sliding-mode control strategy for uncertain systems is introduced in [7]. Moreover, the principle of this technique is to replace the discontinuous switch gain by a fuzzy logic control in the traditional sliding-mode control.

Currently, the design simplicity and robustness are the most important criteria in many applications. This request particularly mobilizes researchers. Whose main concern is the mechanical sensor speed. It is the weakest link in the chain [8]. Indeed, besides the size and difficulty of adaptation when mounting the controller on different types of structures, it is also fragile and expensive.

Received 19 February 2018
Accepted 21 July 2018

Different structures of observers have been proposed in literature. They are very attractive and perform well in an extensive speed range. As seen from the approach based on a model of the machine behaviour applied to observation techniques. There are several categories: extended Kalman filters [9] extended Luenberger observer [10] which guarantees only the local convergence, adaptive methods, and nonlinear observers, such as the sliding-mode observers (SMO) [11], and high-gain observers [12]. In this paper, our focus is on the SMO application on a fuzzy sliding-mode controller. This observer is based on the theory of variable-structure systems. It is well suited for uncertain nonlinear dynamic systems with the same robust layouts as the sliding-mode controllers. In the last two decades, many researchers have proposed different algorithms based on the sliding modes [13] [14]. However, the voltage and current induction-machine models are generally used together to estimate the flux from which the speed is estimated.

SMO reduces the state trajectory of a given system toward a chosen sliding surface and makes it switch to the point of equilibrium. Using a sliding-mode requires mainly two stages, convergence the choice of the surface and establishment of the conditions [15].

The aim of our paper is to show that the estimated speed determines the state of the model. Our results are verified by simulation using the Matlab/Simulink software.

In Section 2 we present a double-star induction machine (DSIM) model. In Section 4 we discuss our control method using the sliding-mode control and fuzzy-logic control. In Section 5 we present the SMO theory. In section 6 our simulation results are analysed and in Section 7 we draw conclusions of our work.

2 DSIM MATHEMATIC MODEL

In the DSIM model there are two three-phase winding systems shifted by an electrical angle of α = 30°. To allow for simplification, the rotor electric circuit is considered to be equivalent to a three-phase winding of a short-circuit occurrence [16].

2.1 Voltage equations

$$\begin{cases} V_{ds1} = R_{s1} i_{ds1} + \dfrac{d}{dt}\phi_{ds1} - \omega_s \phi_{qs1} \\ V_{qs1} = R_{s1} i_{qs1} + \dfrac{d}{dt}\phi_{qs1} + \omega_s \phi_{ds1} \\ V_{ds2} = R_{s2} i_{ds2} + \dfrac{d}{dt}\phi_{ds2} - \omega_s \phi_{qs2} \\ V_{qs2} = R_{s2} i_{qs2} + \dfrac{d}{dt}\phi_{qs2} + \omega_s \phi_{ds2} \\ V_{dr} = 0 = R_r i_{dr} + \dfrac{d}{dt}\phi_{dr} - \omega_{gl} \phi_{qr} \\ V_{qr} = 0 = R_r i_{qr} + \dfrac{d}{dt}\phi_{qr} + \omega_{gl} \phi_{dr} \end{cases} \quad (1)$$

2.2Mechanical equation

$$T_{em} = p \frac{L_m}{L_r + L_m} \left[\phi_{dr} \left(i_{qs1} + i_{qs2} \right) - \phi_{qr} \left(i_{ds1} + i_{ds2} \right) \right] \quad (2)$$

$$J \frac{d\Omega}{dt} = T_{em} - T_L - k_f \Omega \quad (3)$$

2.3Flux equations

$$\begin{cases} \phi_{ds1} = L_{s1} i_{ds1} + L_m \left(i_{ds1} + i_{ds2} + i_{dr} \right) \\ \phi_{qs1} = L_{s1} i_{qs1} + L_m \left(i_{qs1} + i_{qs2} + i_{qr} \right) \\ \phi_{ds2} = L_{s2} i_{ds2} + L_m \left(i_{ds1} + i_{ds2} + i_{dr} \right) \\ \phi_{qs2} = L_{s2} i_{qs2} + L_m \left(i_{qs1} + i_{qs2} + i_{qr} \right) \\ \phi_{dr} = L_r i_{dr} + L_m \left(i_{ds1} + i_{ds2} + i_{dr} \right) \\ \phi_{qr} = L_r i_{qr} + L_m \left(i_{qs1} + i_{qs2} + i_{qr} \right) \end{cases} \quad (4)$$

3 INVERTER VOLTAGE-SOURCE MODELING

In our study, we use two voltage inverters to eliminate certain voltage harmonics and thus minimize the torque ripples and increase the machine efficiency. The voltage inverter is a static converter consisting of switching cells generally with transistors or GTO thyristors for the high powers. They enable the amplitude and frequency of the machine waves to vary from the standard network voltage at the load neutral point given by the following expression:

$$\begin{bmatrix} V_{sa} \\ V_{sb} \\ V_{sc} \end{bmatrix} = \frac{V_d}{3} \begin{bmatrix} 2 & -1 & -1 \\ -1 & 2 & -1 \\ -1 & -1 & 2 \end{bmatrix} \begin{bmatrix} S_1 \\ S_2 \\ S_3 \end{bmatrix} \quad (5)$$

Where:

V_d is the direct voltage and S_1, S_2 and S_3 is the controller signals applied to the switches.

4 SLIDING-MODE CONTROL DESIGN

The sliding mode is a particular system function of a variable structure. The theory of the variable-structure systems and sliding modes is a nonlinear control technique characterized by discontinuous controls.

The basic principle of the sliding-mode control is moving the state trajectory of the system toward surface S(x) = 0 and maintaining it around this surface with switching logic function "U_n". The basic sliding-mode control law is expressed in [17]:

$$U_c = U_{eq} + U_n \quad (6)$$

U_{eq} is obtained with the equivalent-control method. Its principle is based on determination of the behaviour of the system when it is on sliding surface 's', s=0. This control can be either linear or nonlinear.

U_n is a discontinuous control allowing the system to reach and stay on the sliding surface. Generally, the discrete control in the sliding mode can take the form of the relay type given by expression U_n = K.Sign (S (x)).

$$\text{sgn}(S(X)) = \begin{cases} 1 & if \quad S(X) < 0 \\ -1 & if \quad S(X) > 0 \end{cases} \tag{7}$$

For the Lyapunov function to decrease, it suffices to ensure that its derivative is negative:

$$S(X)\,\dot{S}(X) < 0 \tag{8}$$

Using the 'sign' function means that the control between two values is ± K with a theoretically infinite frequency if gain K is very small. The response time will be long if gain K is very large, otherwise, the retry time will be fast, but undesirable oscillations may appear, commonly called "chattering", on the steady-state responses.

One solution to reduce chattering is to incorporate a boundary in the control:

$$U_n = K.F_{sat}\left(\frac{S}{\varepsilon}\right) \tag{9}$$

F_{sat} is a saturation function defined as follows:

$$F_{sat}\left(\frac{S}{\varepsilon}\right) = \begin{cases} \dfrac{S}{\varepsilon} & if \quad \left|\dfrac{S}{\varepsilon}\right| < 1 \\ \text{sgn}\left(\dfrac{S}{\varepsilon}\right) & if \quad \left|\dfrac{S}{\varepsilon}\right| > 1 \end{cases} \tag{10}$$

4.1 FSM control

A fuzzy logic control is introduced to replace the sign function enabling the state trajectory to reach and move along the change surface. A good steady-state dynamics can be achieved by a combination of SMC and FLC [18]. The advantages of the proposed control by using FSM is verified by simulation.

Fig. 1 presents a FSM control scheme replacing expression $U_n=K.F_{sat}(S/\varepsilon)$ by a fuzzy controller.

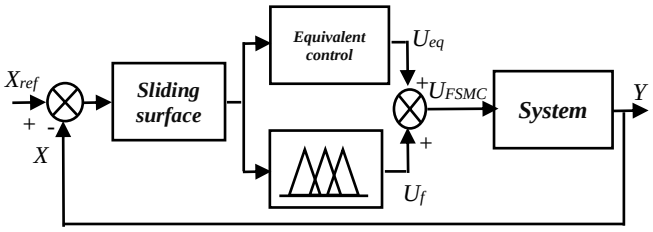

Figure 1. Diagram of the SMC-FLC hybrid control.

As seen from the above, the SMC law explains the control strategy:

"If the error is negative, the output of the system is pushed to the positive direction" [19].

For this, the fuzzy controller can replace term $K.F_{sat}$. This controller has input S (x) and output U_f and its rules serve to establish a connection between S (x) and U_f.

This is interpreted by the rules of the "if ... then" form:

R_1: if S is N Then U_f is N N: Negative
R_2: if S is Z Then U_f is Z Z: Zero
R_3: if S is P Then U_f is P P: Positive

4.2 DSIM FSMC

The synthesis of the SMC law is based on a model obtained after decoupling using the vector control method.

By applying this principle (ϕ_{qr}=0 and ϕ_{dr}= ϕ_r*) to equations (1), (2) and (3), the frame stator voltage equations are:

$$\begin{cases} V_{ds1}^* = R_{s1} i_{ds1} + L_{s1}\dfrac{di_{ds1}}{dt} - \omega_s^*\left(L_{s1} i_{qs1} + T_r \phi_r^* \omega_{gl}^*\right) \\ V_{qs1}^* = R_{s1} i_{qs1} + L_{s1}\dfrac{di_{qs1}}{dt} + \omega_s^*\left(L_{s1} i_{ds1} + \phi_r^*\right) \\ V_{ds2}^* = R_{s2} i_{ds2} + L_{s2}\dfrac{di_{ds2}}{dt} - \omega_s^*\left(L_{s2} i_{qs2} + T_r \phi_r^* \omega_{gl}^*\right) \\ V_{qs2}^* = R_{s2} i_{qs2} + L_{s2}\dfrac{di_{qs2}}{dt} + \omega_s^*\left(L_{s2} i_{ds2} + \phi_r^*\right) \\ \phi_r + T_r \dfrac{d}{dt}\phi_r = L_m\left(i_{ds1} + i_{ds2}\right) \\ \omega_{gl} = \omega_s - \omega_r = \dfrac{L_m}{T_r \phi_r}\left(i_{qs1} + i_{qs2}\right) \end{cases} \tag{11}$$

$$T_{em} = p\frac{L_m}{L_r + L_m}\phi_r\left(i_{qs1} + i_{qs2}\right) \tag{12}$$

$$J\frac{d\Omega}{dt} = T_{em} - T_L - k_f \Omega \tag{13}$$

To cancel the coupling terms, we use a compensation method, The method adds the currents controls i_{ds1}, i_{qs1}, i_{ds2}, i_{qs2} by neglecting the coupling terms, and the obtained output stator voltages are V_{ds1r}, V_{qs1r}, V_{ds2r}, V_{qs2r} for $i^*_{ds1} = i^*_{ds2}$ and $i^*_{qs1} = i^*_{qs2}$.

In our work, the following six sliding surfaces are used:

$$\begin{cases} S(\Omega) = \Omega^* - \Omega \\ S(\phi_r) = \phi_r^* - \phi_r \\ S(i_{ds1}) = i_{ds1}^* - i_{ds1} \\ S(i_{qs1}) = i_{qs1}^* - i_{qs1} \\ S(i_{ds2}) = i_{ds2}^* - i_{ds2} \\ S(i_{qs2}) = i_{qs2}^* - i_{qs2} \end{cases} \tag{14}$$

By using equation systems (3), (6) and (9), the obtained control laws are:

4.2.1 The Speed controller:

$$S(\omega_r)\dot{S}(\omega_r) < 0 \quad \Rightarrow \quad i_{qs}^* = i_{qseq} + i_{qsn} \tag{15}$$

With: $i_{qs} = i_{qs1} + i_{qs2}$ *and* $\omega_r = p\Omega$

$$i_{qseq} = \frac{j}{p^2}\frac{L_r + L_m}{L_m \phi_r^*} + \left[\omega_r^* \frac{k_f}{j}\omega_r + \frac{p}{j}T_L\right] \tag{16}$$

$$i_{qsn} = \begin{cases} \dfrac{K_\omega}{\varepsilon_\omega} S(\omega_r) & if \quad \left|\dfrac{S(\omega_r)}{\varepsilon_\omega}\right| \le 1 \\ K_\omega \,\text{sgn}(S(\omega_r)) & if \quad \left|\dfrac{S(\omega_r)}{\varepsilon_\omega}\right| > 1 \end{cases} \tag{17}$$

4.2.2 The Flux controller:

$$S(\phi_r)\dot{S}(\phi_r)<0 \quad \Rightarrow \quad i_{ds}^{*}=i_{dseq}+i_{dsn} \tag{18}$$

at $i_{ds}=i_{ds1}+i_{ds2}$

$$i_{dseq}=\frac{L_r+L_m}{R_r L_m}+\left[p\phi_r^{*}+\frac{R_r}{L_r+L_m}\phi_r\right] \tag{19}$$

$$i_{dsn}=\begin{cases}\dfrac{K_\phi}{\varepsilon_\phi}S(\phi_r) & if \quad \left|\dfrac{S(\phi_r)}{\varepsilon_\phi}\right|\le 1\\ K_\phi \operatorname{sgn}(S(\phi_r)) & if \quad \left|\dfrac{S(\phi_r)}{\varepsilon_\phi}\right|>1\end{cases} \tag{20}$$

4.2.3 The Stator current controller:

$$\begin{cases}S(i_{ds1})\dot{S}(i_{ds1})<0\Rightarrow V_{ds1}^{*}=V_{ds1eq}+V_{ds1n}\\ S(i_{qs1})\dot{S}(i_{qs1})<0\Rightarrow V_{qs1}^{*}=V_{qs1eq}+V_{qs1n}\\ S(i_{ds2})\dot{S}(i_{ds2})<0\Rightarrow V_{ds2}^{*}=V_{ds2eq}+V_{ds2n}\\ S(i_{qs2})\dot{S}(i_{qs2})<0\Rightarrow V_{qs2}^{*}=V_{qs2eq}+V_{qs2n}\end{cases} \tag{21}$$

With

$$\begin{cases}V_{ds1eq}=L_{s1}i_{ds1}^{*}+R_{s1}i_{ds1}-\omega_s^{*}\left[L_{s1}i_{qs1}+T_r\phi_r^{*}\omega_{gl}^{*}\right]\\ V_{qs1eq}=L_{s1}i_{qs1}^{*}+R_{s1}i_{qs1}+\omega_s^{*}\left[L_{s1}i_{ds1}+\phi_r^{*}\right]\\ V_{ds2eq}=L_{s2}i_{ds2}^{*}+R_{s2}i_{ds2}-\omega_s^{*}\left[L_{s2}i_{qs2}+T_r\phi_r^{*}\omega_{gl}^{*}\right]\\ V_{qs2eq}=L_{s2}i_{qs2}^{*}+R_{s2}i_{qs2}+\omega_s^{*}\left[L_{s2}i_{ds2}+\phi_r^{*}\right]\end{cases} \tag{22}$$

And

$$\begin{cases}V_{ds1n}=K_{d1}F_{sat}\left(\dfrac{S(L_{ds1})}{\varepsilon}\right)\\ V_{qs1n}=K_{q1}F_{sat}\left(\dfrac{S(L_{qs1})}{\varepsilon}\right)\\ V_{ds2n}=K_{d2}F_{sat}\left(\dfrac{S(L_{ds2})}{\varepsilon}\right)\\ V_{qs2n}=K_{q2}F_{sat}\left(\dfrac{S(L_{qs2})}{\varepsilon}\right)\end{cases} \tag{23}$$

To verify the system stability condition, gains K_ω, K_φ, K_d and K_q should be positive by selecting the appropriate values. In order to reduce chattering, three FSMCs are used following the "If…then" rule, max-min inference mechanism and center of gravity defuzzyfier. FSMCs are chosen as follows [20]:

$$\begin{cases}i_{qs}^{*}=i_{qseq}+i_{qsf}\\ i_{ds}^{*}=i_{dseq}+i_{dsf}\\ V_{ds1}^{*}=V_{ds1eq}+V_{ds1f}\\ V_{qs1}^{*}=V_{qs1eq}+V_{qs1f}\\ V_{ds2}^{*}=V_{ds2eq}+V_{ds2f}\\ V_{qs2}^{*}=V_{qs2eq}+V_{qs2f}\end{cases} \tag{24}$$

Fig. 2 shows the membership functions of input S(x) and output Un:

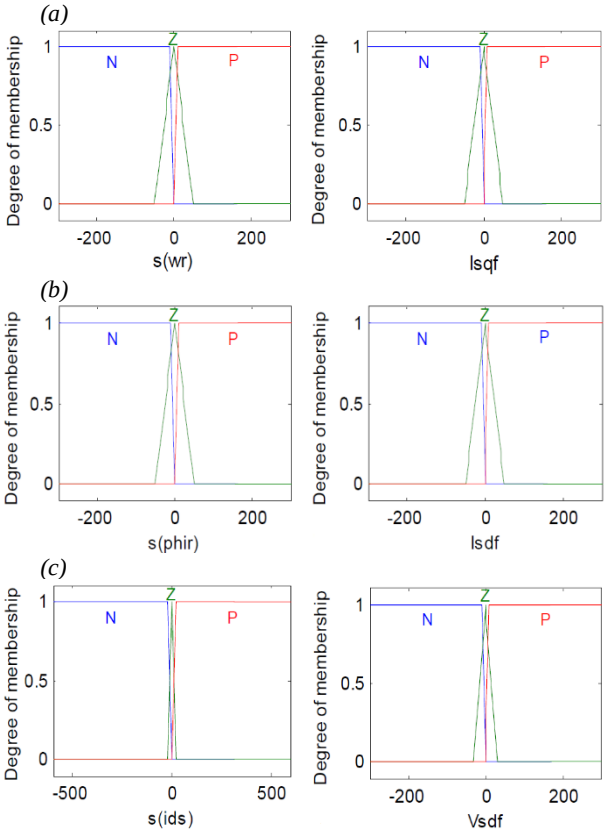

Figure 2. FSMC input/output membership functions of (a) speed, (b) flux, (c) current.

5 SMO

SMO to be used in the rotor speed estimation should be robust (invariance to parametric variations) and simple.

In literature, generally, the voltage and current models of the induction machine are used together to estimate the flux from which the speed is estimated [21], [22].

If the system is observable, the objective of the observer is to give the best estimate of the state variables from the measurements on output y and on input u_s.

The observer is defined as follows [23]:

$$\dot{\hat{x}}=\hat{f}(\hat{x},y,u,t)+u_s \tag{25}$$

Where:

x is of the same dimension as x (n);

f is the estimation model;

u_s is the vector defined by,

$$u_s=\left[G_1 smooth\ (S_1)\ G_2 smooth\,(S_2)\ \ldots\ \ G_n smooth\ (S_r)\right]^t \quad (26)$$

The sign function is replaced by a continuous approximation near the sliding surface. From the methods reducing the effect of the sign function we use the smooth function of the dead zone to filter high frequencies and eliminate the chattering phenomenon and generated transient electromagnetic torque in the dynamic and low-speed profiles [24].

The smooth function used to eliminate the chattering phenomenon is determined with the following relation:

$$smooth(S)=\frac{S}{|S|+\xi} \quad (27)$$

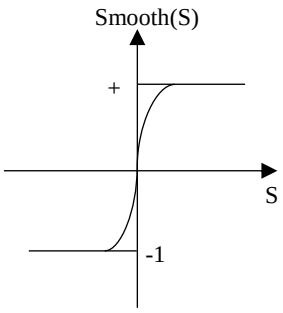

Figure 3. Smooth function.

$$\left[S_1\quad S_2\quad \ldots\quad S_r\right]^t = S=\left[y-\hat{y}\right]$$

Surface vector S = 0 is attractive if:

$$S_i\,\dot{S}_i<0\quad for\quad i=1,r$$

The objective is to observe the speed (Ω) based on the stator currents and voltages which are easily measurable.

The system of equations (11), (12) and (13) can be rewritten as two subsystems:

$$\begin{cases}\dfrac{di_{ds1}}{dt}=\dfrac{1}{L_{s1}}v_{ds1}-\dfrac{R_{s1}}{L_{s1}}i_{ds1}+\omega_s\left(\dfrac{L_r}{R_r}.\phi_r.\omega_{gl}+L_{s1}.i_{qs1}\right)\\ \dfrac{di_{ds2}}{dt}=\dfrac{1}{L_{s2}}v_{ds2}-\dfrac{R_{s2}}{L_{s2}}i_{ds2}+\omega_s\left(\dfrac{L_r}{R_r}.\phi_r.\omega_{gl}+L_{s2}.i_{qs2}\right)\\ \dfrac{d\phi_r}{dt}=-\dfrac{1}{T_r}\phi_r+\dfrac{L_m}{T_r}(i_{ds1}+i_{ds2})\end{cases} \quad (28)$$

$$\begin{cases}\dfrac{di_{qs1}}{dt}=\dfrac{1}{L_{s1}}v_{qs1}-\dfrac{R_{s1}}{L_{s1}}i_{qs1}-\omega_s\left(\phi_r+L_{s1}.i_{ds1}\right)\\ \dfrac{di_{qs2}}{dt}=\dfrac{1}{L_{s2}}v_{qs2}-\dfrac{R_{s2}}{L_{s2}}i_{qs2}-\omega_s\left(\phi_r+L_{s2}.i_{ds2}\right)\\ \dfrac{d\Omega}{dt}=\dfrac{p}{J}\dfrac{L_m}{L_m+L_r}.\phi_r.(i_{qs1}+i_{qs2})-\dfrac{K_f}{J}\Omega-\dfrac{1}{J}T_L\end{cases} \quad (29)$$

To estimate the speed, only subsystem (29) is used. It is correct for most applications [25] [26].

To estimate the speed from the model described by subsystem (29), the rotor flux should be estimated.

The SMO model is given by:

$$\begin{cases}\dfrac{d\hat{i}_{qs1}}{dt}=\dfrac{1}{L_{s1}}v_{qs1}-\dfrac{R_{s1}}{L_{s1}}\hat{i}_{qs1}-\omega_s\left(i_{ds1}+\dfrac{1}{L_{s1}}\hat{\phi}_r\right)+G_1 smooth\left(\tilde{i}_{qs}\right)\\ \dfrac{d\hat{i}_{qs2}}{dt}=\dfrac{1}{L_{s2}}v_{qs2}-\dfrac{R_{s2}}{L_{s2}}\hat{i}_{qs2}-\omega_s\left(i_{ds2}+\dfrac{1}{L_{s2}}\hat{\phi}_r\right)+G_1 smooth\left(\tilde{i}_{qs}\right)\\ \dfrac{d\hat{\Omega}}{dt}=\dfrac{p}{J}\dfrac{L_m}{L_m+L_r}.\hat{\phi}_r.(\hat{i}_{qs1}+\hat{i}_{qs2})-\dfrac{K_f}{J}\hat{\Omega}-\dfrac{p}{J}\hat{T}_L++G_2 smooth\left(\tilde{i}_{qs}\right)\\ \dfrac{d\hat{T}_L}{dt}=G_3 smooth\left(\tilde{i}_{qs}\right)\\ \dfrac{d\hat{\phi}_r}{dt}=\dfrac{L_m}{T_r}(i_{ds1}+i_{ds2})-\dfrac{1}{T_r}\hat{\phi}_r\\ smooth\left(\tilde{i}_{qs}\right)=\dfrac{\tilde{i}_{qs}}{|\tilde{i}_{qs}|+\xi}\qquad with\qquad \tilde{i}_{qs}=(i_{qs1}+i_{qs2})-(\hat{i}_{qs1}+\hat{i}_{qs2})\end{cases}$$

G_1, G_2 and G_3 are the SMO gains.

The following block diagram illustrates FSMC with no speed sensor of a double-star induction motor equipped with SMO, fig. 4:

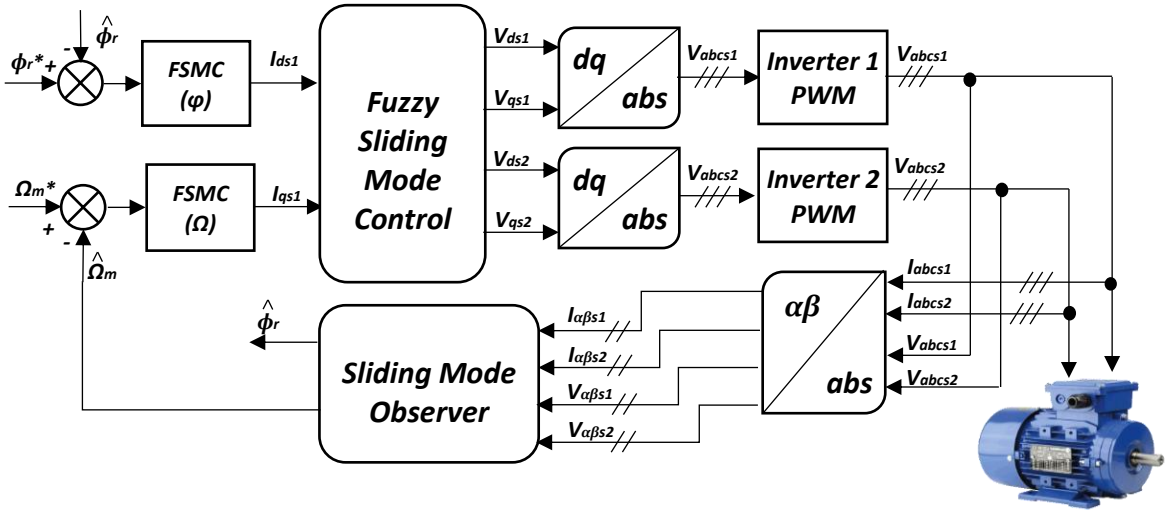

Figure 4. DSIM FSMC block diagram equipped with SMO.

6 SIMULATION RESULT

To test the static and dynamic SMO performance, DSIM fed by two voltage inverters is used. In our simulations, the load disturbance of T_L = 14 N.m is applied between 1s and 2s with the speed reversal at t = 3s.

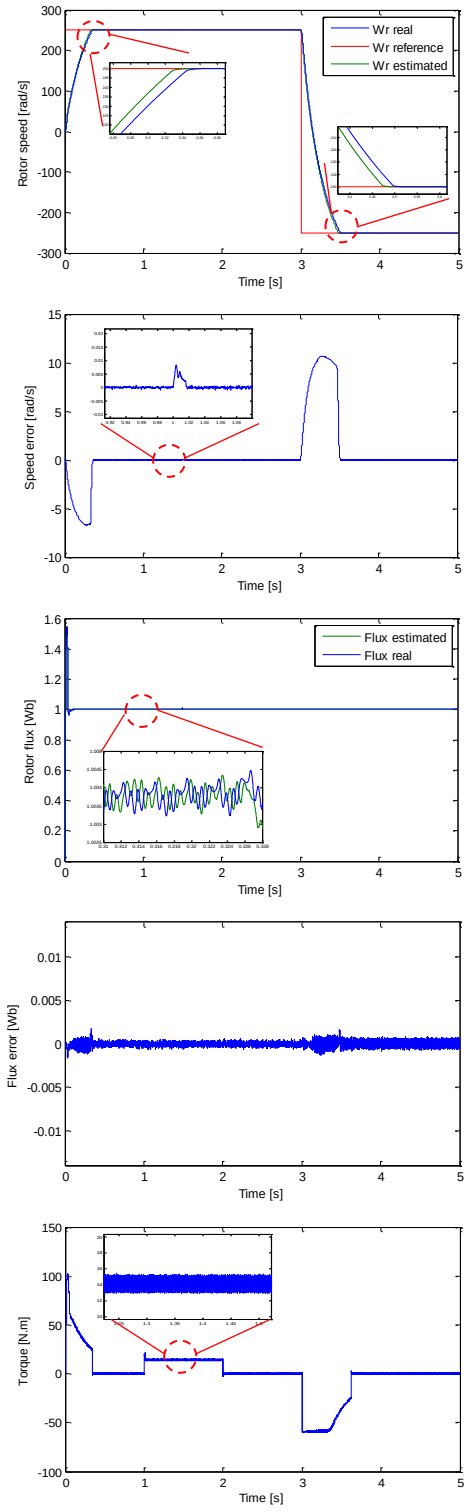

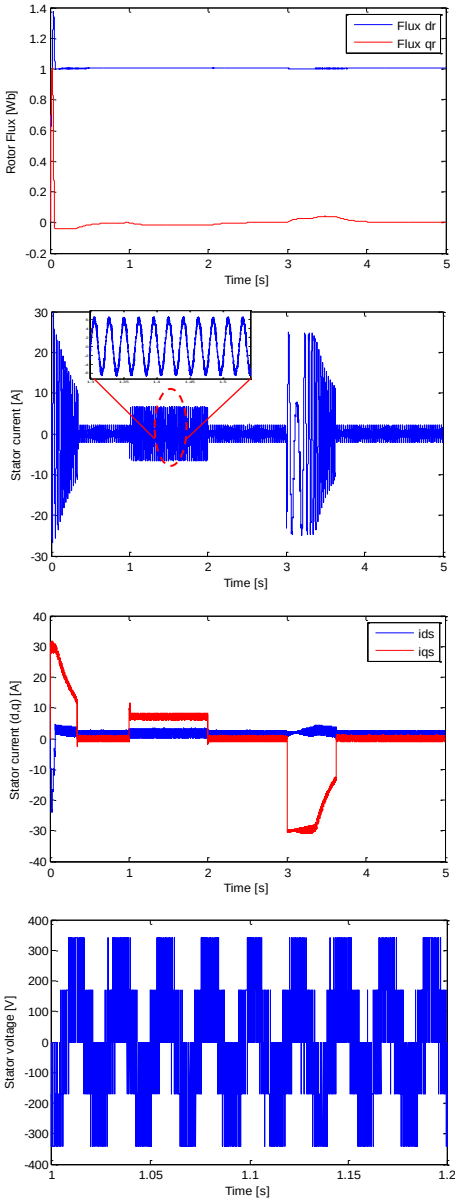

Figure 5. Simulation results of a real and estimated speed, real and estimated stator flux, torque, stator current and stator voltage of a DSIM sensorless control.

Fig. 5 illustrates the electromagnetic torque, stator-phase current, real and estimated speed, real and estimated flux and the corresponding estimation errors of a FSMC with no speed sensor. By using the sliding mode technique, the observer is applied to DSIM for different speed references.

The simulation results show a good FSMC performance (speed, stability and precision) as well as an improvement made by FSMC compared to SMC in terms of reduced chattering effect (variations in the torque and stator flux) and absence of disturbances.

The speed reversal from the positive to the negative value (250 rad/s; –250 rad/s) is made in order to show that FSMC operates at different speed points. During the reversal stage, the speed controller shows a similar

behaviour as at the starting-up stage by operating the system at the physical limit. This can be clearly seen by the torque response. The speed and the torque response show a good dynamic and reference tracking during the transient and steady state. The magnitude and the trajectory illustrate that the flux takes a few steps before reaching the reference value (1Wb). The stator current shows a good sinusoid waveform.

Comparing the simulation results of the measurable and observable magnetic and mechanical DSIM magnitudes using SMO controlled by FSMC, we see that the used observer performs a good speed and flux tracking with an unimportant dynamic error in the transient state, and the static error is practically zero in the steady state. This is due to the chosen parameters of the observer gains. To avoid variations in the transient state, it is necessary to choose another combination to ensure the observer convergence. Note also that SMO does not affect the control behaviour and dynamics when using the load torque. It can be conclude thus that the presence of the observer does not affect the FSMC behaviour.

6.1 Speed-variation test

This test comprises all the previous tests. Fig. 6 shows the SMO rotor speed estimation under a variable reference from zero to a low speed (50 rad/s) and from a medium (150 rad/s) to a high-speed value (250 rad/s). The estimation error is given in fig. 6.

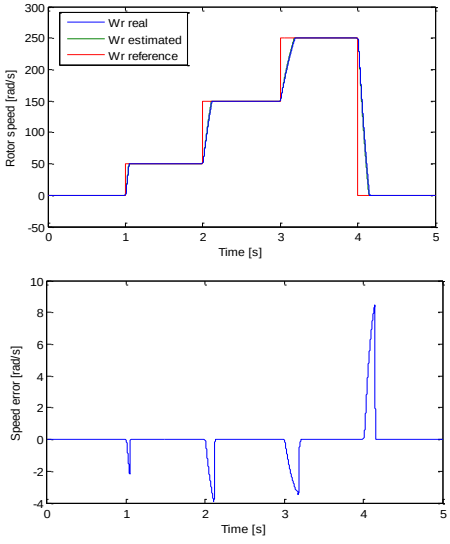

Figure 6. Real and estimated speed trajectory for different speeds.

This test shows a perfect tracing and an accurate speed. It can be concluded that SMO provides a considerable error only at a variable state and eliminates it at a steady state.

6.2 A Comparison between the SMC and FSMC chattering effect

Fig. 7 shows a comparison between the SMC and FSMC chattering effect.

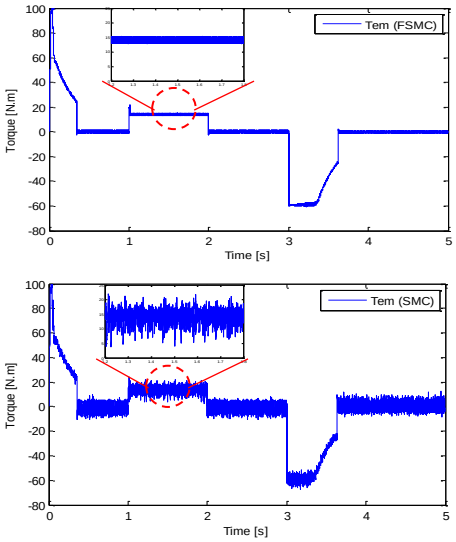

Figure 7. Comparison between the SMC and FSMC chattering effect.

A comparison between the torques obtained with the two modes shows that using FSM performs a better control than when using SM in terms of the reduced chattering effect.

7 CONCLUSION

The paper presents a performance enhancement by using FSMC decoupled by a control vector. To solve different drawbacks of the PI controllers, a hybrid control technique combining FLC and SMC is presented. The vector control is applied to create a decoupled flux and torque and FSMC to limit the disadvantages of the PI controllers enabling a robust control and reducing the chattering effect.

To synthesize the software sensor, minimize the cost of assembly and reduce the number of physical sensors, SMO is developed. The simulation results prove that it eliminates the static error and provides a more precise estimation in the steady state. The chattering effect is reduced by using a smooth switching function. The speed-variation test shows that the sensorless control scheme preserves its performance even in this region. It can be concluded that when using SMO a considerable error occurs only in a variable state and these is none in a steady state.

The proposed method can be readily used in practice. In our further research, our theory will be experimental by validated.

APPENDIX

The machine parameter values used for the simulation are:

Table 1. DSIM parameters.

Parameters	Values	Parameters	Values
Pn [Kw]	4.5	Vn [V]	220
Rr [Ω]	2.12	Lr [H]	0.006
Rs1 [Ω]	1.86	Rs2 [Ω]	1.86
Ls1 [H]	0.011	Ls2 [H]	0.011
P	1	Lm [H]	0.3672
J [Kg.m²]	0.065	kf [N.m.s/rad]	0.001

REFERENCES

[1] A. Meroufel, S.Massoum, A. Bentaallah, P. Wira, F.Z Belaimech, A. Massoum, "Double star induction motor direct torque control with fuzzy sliding mode speed controller", Rev. Roum. Sci. Techn– Électrotechn and Énerg, 62 (1), pp. 31–35, Bucarest, 2017.

[2] K. Sahraoui, K. Kouzi, A. Ameur, "Optimization of MRAS based Speed Estimation for Speed Sensorless Control of DSIM via Genetic Algorithm", Electrotehnica, Electronica, Automatica (EEA), 65 (3), pp. 156-162, 2017.

[3] A. Boucheta, I. K. Bousserhane, A. Hazzab, "Fuzzy sliding mode controller for linear induction motor control", Rev. Roum. Sci. Techn. – Électrotechn. et Énerg., 54 (4), Bucarest, pp. 405–414, 2009.

[4] A. Ayadi, S. Hajji, M. Smaoui, A. Chaari, M. Farza, "Experimental sensorless control for electropneumatic system based on high gain observer and adaptive sliding mode control", Int J Adv Manuf Technol, Springer, pp.1-14, 2017.

[5] Xizheng Z, Yaonan W, Minsheng Y. "Fuzzy sliding mode control for induction motors with robust H inf performance", Information technology journal, 10 (7), pp. 1351 – 1358, 2011.

[6] Y. Yuntao, L. Yan, "A Novel Sensorless Fuzzy Sliding-Mode Control of Induction Motor", International Journal of Control and Automation, 8 (9), pp. 1-10, 2015.

[7] A. Saghafinia, H. Ping, M. Uddin, K. Gaeid, "Adaptive Fuzzy Sliding-Mode Control Into Chattering-Free IM Drive", IEEE Transactions on Industry Applications, 51 (1), pp. 692-701, 2015.

[8] M. H. Lazreg, A. Bentaallah, "Speed sensorless vector control of double star induction machine using reduced order observer and MRAS estimator", IEEE International Conference on Electrical Engineering (ICEE-B), Boumerdes, Algeria, 29-31 October, 2017.

[9] M. A. Usta, H. I. Okumus, H. Hakan Kahveci, "A simplified three-level SVM-DTC induction motor drive with speed and stator resistance estimation based on extended Kalman filter", Electr Eng, Springer, pp. 1-14, 2016.

[10] A. Ahmed, Z. Diab, "Implementation of a novel full-order observer for speed sensorless vector control of induction motor drives", Electr Eng, Springer, pp. 1-15, 2016.

[11] A. Ammar, A. Bourek, A. Benakcha, "Robust SVM-direct torque control of induction motor based on sliding mode controller and sliding mode observer", Frontiers in Energy, pp. 1-14, 2017.

[12] I. Haj Brahim, H. Soufien, A. Soufien, "Backstepping Controller Design using a High Gain Observer for Induction Motor", International Journal of Computer Applications, 23 (3), pp. 1-6, 2011.

[13] L. Jinkun, W. Xinhua, "Advanced Sliding Mode Control for Mechanical Systems - Design, Analysis and MATLAB Simulatio", Tsinghua University Press, Beijing and Springer-Verlag Berlin Heidelberg, pp. 166 – 168, 2012.

[14] H. Khouidmi, A. Massoum, "Reduced-Order Sliding Mode Observer-based Speed Sensorless Vector Control of Double Stator Induction Motor", Acta Polytechnica Hungarica, 11 (6), pp. 229-249, 2014.

[15] Z. Xiaoguang, L. Zhengxi, "Sliding-mode observer-based mechanical parameter estimation for permanent magnet synchronous motor", IEEE Trans. Power Electron, 31(8), pp. 5732–5745, 2016.

[16] Z. Tir, O. P. Malik, A. M. Eltamaly, "Fuzzy logic based speed control of indirect field oriented controlled Double Star Induction Motors connected in parallel to a single six-phase inverter supply", Electric Power Systems Research, elsevier, 134, pp. 126–133, 2016.

[17] A. Ammar, A. Bourek, A. Benakcha, "Nonlinear SVM-DTC for induction motor drive using input-output feedback linearization and high order sliding mode control", ISA Transactions, 67, pp. 428-442, 2017.

[18] Lekhchine S, Bahi T, Abadlia I, Bouzeria H. PV-battery energy storage system operating of asynchronous motor driven by using fuzzy sliding mode control, international journal of hydrogen energy, Elsevier, pp. 1-9, 2016.

[19] F. Benchabane, A. Titaouine, O. Bennis, K. Yahia, D. Taibi, "Sensorless fuzzy sliding mode control for permanent magnet synchronous motor fed by AC/DC/AC converter", Int J Syst Assur Eng Manag, 3(3), pp. 221–229, 2012.

[20] R. Sadouni, A. Meroufel, S. Djriou, A. Kheldoun, "A Fuzzy Sliding Mode Robust Control for a Field Oriented Dual Star Induction Machine Fed by Photovoltaic power supply with MPPT algorithm", The Mediterranean Journal of Measurement and Control, 10 (4), pp. 1 – 10, 2016.

[21] A. Glumineau, J. Morales, "Sensorless AC Electric Motor Control (Robust Advanced Design Techniques and Applications)", Advances in Industrial Control, Springer, pp. 1-6, 2015.

[22] M. Moutchou, H. Mahmoudi, "Sensorless Exact Input-Output Linearization Control of the Induction Machine, Based on Parallel Stator Resistance and Speed MRAS Observer, with a Flux Sliding Mode Observer", International Journal on Electrical Engineering and Informatics, 6 (2), pp. 324 – 341, 2014.

[23] A. Hosseyni, R. Trabelsi, M.F. Mimouni, A. Iqbal, R. Alammari, "Sensorless sliding mode observer for a five-phase permanent magnet synchronous motor drive", ISA Transactions, Elsevier J. 58, pp. 462–473, 2015.

[24] O. Saadaoui, A. Khlaief, M. Abassi, A. Chaari, M. Boussak, "A sliding mode observer for high-performance sensorless control of PMSM with initial rotor position detection", International Journal of Control, Taylor & Francis, 2016.

[25] R. Kianinezhad, B. Nahid, F. Betin, G.A. Capolino, "Observer-Based Sensorless Field-Oriented Control of Induction Machines", IEEE Trans. on Ind. Appl, 71, pp. 1381-1385, 2004.

[26] R. Kianinezhad, B. Nahid-Mobarakeh, F. Betin, G.A. Capolino, "Sensorless fieldoriented control for six-phase induction machines", IEEE Trans. on Ind. Appl., Vol. 71, pp. 999-1006, 2005.

Mohamed Haithem Lazreg received his Master degree in Electrical Engineering in 2015 from the Djillali Liabes University, Sidi Bel Abbes, Algeria. He is currently a PhD student at the same University and a member of the ICEPS (Intelligent Control Electrical Power System) Laboratory. His research interests are in advanced control of ac drives and sensorless, intelligent artificial control.

Abderrahim Bentaallah received his BS, MSc and Ph.D degrees in Electrical engineering from the Djillali Liabes University, Sidi Bel-Abbes, Algeria in 1991, 2005 and 2009, respectively. He is currently Professor of electrical engineering at this University. He is a member of ICEPS. His research interest is in robust control of electric machines.